THE REACTIONS OF Cl AND ClO WITH THE NO_3 RADICAL

R.A. COX, R.A. BARTON, E. LJUNGSTROM * and D.W. STOCKER **
Environmental and Medical Sciences Division, AERE Harwell, Oxon, UK

Received 11 April 1984; in final form 3 May 1984

The photolysis of Cl_2 in the presence of $ClONO_2$ was used as a source of NO_3 radicals via the reaction $Cl + ClONO_2 \rightarrow Cl_2 + NO_3$. The kinetic growth and decay of NO_3 were measured using time-resolved absorption at 662 nm. The reactions $Cl + NO_3 \rightarrow ClO + NO_2$ (7) and $ClO + NO_3 \rightarrow ClOO + NO_2$ (8) appeared to be important, with $k_7 = (7.6 \pm 1.1) \times 10^{-11}$ and $k_8 = (4.0 \pm 1.7) \times 10^{-13}$ cm^3 molecule^{-1} s^{-1} at 296 K. A value of 1.63×10^{-17} cm^2 molecule^{-1} was determined for the absorption cross section of NO_3 at 662 nm.

1. Introduction

It has been recognised for some time that the nitrate radical plays an important role in atmospheric NO_x chemistry. Its principal route of formation is the reaction of NO_2 with ozone [1]:

$$NO_2 + O_3 \rightarrow NO_3 + O_2 \,. \qquad (1)$$

In daylight, NO_3 is rapidly photolysed.

$$NO_3 + h\nu \rightarrow NO + O_2 \,, \qquad (2a)$$

$$\rightarrow NO_2 + O \,, \qquad (2b)$$

but also reacts rapidly with NO and NO_2:

$$NO_3 + NO \rightarrow 2NO_2 \,, \qquad (3)$$

$$NO_3 + NO_2 + M \rightarrow N_2O_5 + M \,. \qquad (4)$$

NO_3 radicals have recently been identified as potential attacking species in the atmospheric oxidation of organic molecules, particularly aromatic hydrocarbons [2]. Assessment of the importance of this process as well as the rate of oxidation of NO_2 via (1) requires definition of the steady-state concentration of NO_3. Accurate kinetic and photochemical data for the reactions controlling NO_3 concentration in the atmosphere are therefore needed.

Until recently, most of the photochemical and kinetic information concerning NO_3 reactions was due to Johnston and co-workers [3,4], who investigated the chemistry of the NO_2–O_3–N_2O_5 system. This work provided indirect determinations of rate coefficients for a number of elementary reactions of NO_3 and also the absorption cross section σ and quantum yields for photodissociation of NO_3 in its broad, structured visible-absorption band. Mitchell et al. [5] have also used the $NO_2 + O_3$ reaction as a source of NO_3, and obtained an estimate of the absorption cross section in the 0–0 vibronic band at 622 nm. Their result was approximately 50% lower than the most recent value from Marinelli et al. [4].

Very recently, Ravishankara and Wine [6] have reported measurements of the NO_3 absorption cross sections in the region 565–673 nm. NO_3 was generated in the reaction of F atoms with HNO_3 in a discharge flow system, and its concentration determined by chemical titration with NO, reaction (3). The value of σ at the peak of the 662 nm band showed good agreement with the result of Marinelli et al. [4].

Recent work on the chemistry of chlorine nitrate, $ClONO_2$ [7,8], has shown that the reaction of Cl with $ClONO_2$ is much faster than hitherto believed. This offers a potentially useful source of NO_3 radicals by the reaction

---

* Chalmers University, Gotenborg, Sweden.
** Department of Chemistry, University of Birmingham.

$$\mathrm{Cl} + \mathrm{ClONO_2} \rightarrow \mathrm{Cl_2} + \mathrm{NO_3} \qquad (5)$$

$$(k_5 = 1.12 \times 10^{-11}\ \mathrm{cm^3\ molecule^{-1}\ s^{-1}\ at\ 298\ K})\,.$$

In the present paper, we describe experiments in which photolysis of Cl_2 at 350 nm was employed to generate Cl atoms in the presence of $ClONO_2$. NO_3 formation and decay was monitored in absorption at 662 nm, and observations of NO_3 kinetics enabled a determination of the absorption cross section σ_{NO_3} at 662 nm and rate coefficients for reactions of Cl and ClO with NO_3, which are proposed to explain the kinetics of NO_3 removal in the system.

2. Experimental

The experiments were performed in a 120 cm long jacketed quartz reaction cell at atmospheric pressure and 296 K. The cell was surrounded by fix fluorescent "Blacklights" (Philips TL 40/08), any number of which could be activated by an electronically switched 250 V dc power supply for a preset period. The spectral monitoring beam from either a deuterium lamp or a tungsten–halogen lamp passed along the cell before dispersion on an 0.75 m Spex monochromator and detection on a photomultiplier. The photomultiplier signal was recorded on a fast digital multichannel scaler, giving time-resolved absorption profiles with millisecond time resolution. The details of this device have been reported elsewhere [9].

The reaction cell was filled with a mixture of Cl_2 ($\approx 10^{15}$ molecule cm^{-3}) and chlorine nitrate ($\approx 2 \times 10^{14}$ molecule cm^{-3}) in N_2 diluent from a flow manifold at atmospheric pressure. $ClONO_2$ was introduced by passing part of the diluent through a bubbler containing a sample of liquid $ClONO_2$ at −60°C. The $ClONO_2$ was prepared using the reaction of chlorine monoxide with nitrogen pentoxide. Cl_2 was taken from a cylinder (BOC 5% Cl_2 in N_2) through a flowmeter a needle valve. Concentrations of Cl_2 and $ClONO_2$ in the reaction cell were determined by absorption at 350 nm and 220 nm, respectively, using cross sections of 1.85×10^{-19} and 3.2×10^{-18} cm^2, respectively. For the kinetics experiments, the flow through the vessel was stopped and photolysis performed on static gas mixtures. Time-resolved absorption during a selected period of illumination followed by an equal period of dark chemistry was recorded.

The rate of photolysis of Cl_2 for any combination of the six lamps was determined in separate experiments in which the rate of decay of Cl_2 in the presence of excess H_2 and O_2 was monitored [10]. The rate constant determined for the photodissociation reaction

$$\mathrm{Cl_2} + h\nu \rightarrow 2\mathrm{Cl} \qquad (6)$$

was $k_6 = 8.84 \times 10^{-4}\ s^{-1}$ per lamp.

3. Results

Fig. 1 shows a typical absorption (at 662 nm) versus time recording in the photolysis of a static mixture containing initially 1.36×10^{15} molecule cm^{-3} Cl_2 and 2.7×10^{14} molecule cm^{-3} $ClONO_2$. It can be seen that NO_3 initially increases steadily on photolysis but then levels off to a steady state. On cessation of photolysis, the radical decays rather slowly, taking about 30 s for 97% decay.

The absorption cross section for NO_3 was determined from measurement of the initial rate of increase in absorption in experiments covering a 20-fold range of NO_3 production rate, obtained by varying the quantity $Nk_6[Cl_2]$ (N is the number of photolysis lamps). Based on the assumption that each Cl atom produced photolytically yields an NO_3 radical, the average of all the data gave a value of

$$\sigma_{NO_3} = (1.63 \pm 0.15) \times 10^{-17}\ \mathrm{cm^2\ molecule^{-1}}\,.$$

The kinetic behaviour of NO_3 during photolysis

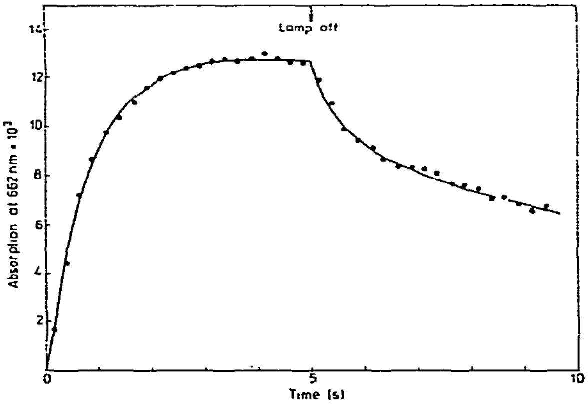

Fig. 1. Concentration behaviour of NO_3 from absorption at 662 nm.

and in the dark was also analysed. Examination of fig. 1 showed that the rise to steady state followed first-order kinetics fairly closely, i.e. NO_3 is formed at a constant rate during illumination and is removed by a pseudo-first-order process. The first-order rate constants, k^1, for the reaction $NO_3(+X) \rightarrow$ products, where X is a reactant present at constant (steady-state or excess) concentration or an absorbed photon, were determined from plots of $\ln[A_{max}/(A_{max} - A_t)]$ versus time (A is the absorption of NO_3). The plots were linear up to at least three half-lives, giving values of k^1 in the range 0.25–$3.0\ s^{-1}$.

Direct photolysis can be ruled out as a major loss process for NO_3, since it would require a photodissociation rate approximately 1000 greater than that for Cl_2 in the 350 nm region to give the required value of k^1. Although NO_3 may absorb in this region, a cross section of the order of 10^{-16} cm^2 molecule^{-1} is unreasonably large. However, k^1 did seem to vary systematically with both light intensity and $ClONO_2$ concentration. Fig. 2 shows a plot of k^1 against the ratio $2k_6[Cl_2]/[ClONO_2]$ for initial conditions. The plot was reasonably linear, indicating that the concentration of X was proportional to the rate of Cl atom production and inversely proportional to chlorine nitrate concentration. This observation rules out reaction of NO_3 with $ClONO_2$, which would show the opposite dependence on $[ClONO_2]$ to that observed. The most likely candidate for X appears to be Cl atoms, since a steady state involving reactions (5) and (6) would give

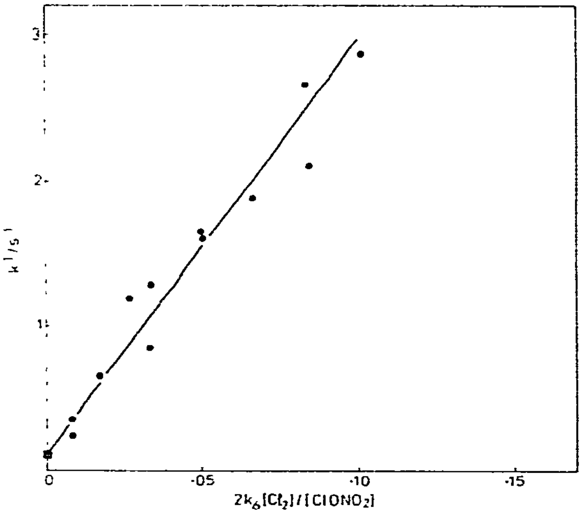

Fig. 2. Plot of first-order rate coefficient for NO_3 removal against the ratio $2k_6[Cl_2]/[ClONO_2]$.

$$[Cl] = 2k_6[Cl_2]/k_5[ClONO_2] . \qquad (i)$$

If $k^1 = nk_7[Cl]$, where n is the number of NO_3 radicals removed following the reaction

$$Cl + NO_3 \rightarrow \text{products} , \qquad (7)$$

then the slope of the plot in fig. 2 (=27.2 ± 2.6) gives the rate-constant ratio nk_7/k_5. The value for k_5 quoted above leads to $nk_7 = (30.5 \pm 4.4) \times 10^{-11}$ cm^3 molecule^{-1} s^{-1} (error = 2 standard deviations based on the error of the slope of fig. 2 and the uncertainty in k_5).

The observed first-order kinetics and the above analysis require that the occurrence of reaction (7) does not lead to net loss of Cl atoms. If reaction (7) was a sink for Cl, both the rate of production of NO_3 and the pseudo-first-order removal rate coefficient k^1 would decrease with time, giving rise to complex kinetic behaviour. A plausible mechanism to explain the observed behaviour involves the following elementary processes:

$$Cl + NO_3 \rightarrow ClO + NO_2 , \qquad \Delta H^0 = -57\ \text{kJ mol}^{-1}, \qquad (7)$$

$$ClO + NO_3 \rightarrow ClOO + NO_2 , \qquad \Delta H^0 = -46\ \text{kJ mol}^{-1}, \qquad (8)$$

$$ClOO + M \rightarrow Cl + O_2 + M , \qquad (9)$$

$$NO_2 + NO_3 + M \rightarrow N_2O_5 + M . \qquad (4)$$

Of these reactions, (9) and (4) are reasonably well established and the rate coefficients at 1 atm pressure can be calculated from the pressure dependences given in the recent NASA evaluation [11]. Reactions (7) and (8) do not appear to have been characterised previously but both are reactions between two radical/atomic species and therefore likely to be relatively rapid at ambient temperature.

In the above scheme, 4 NO_3 molecules are removed in the sequence (7) + (8) + 2 X (4), i.e. $n = 4$. This gives a value of

$$k_7 = (7.6 \pm 1.1) \times 10^{-11}\ \text{cm}^3\ \text{molecule}^{-1}\ \text{s}^{-1}$$

at 296 K.

The steady-state concentration of NO_3 reached during illumination and controlled by reactions (4)–(9) is given by

$$[NO_3]_s = \frac{k_5[Cl][ClONO_2]}{k_7[Cl] + k_8[ClO] + k_4[NO_2]} . \qquad (ii)$$

Furthermore, if Cl, ClO and NO_2 are also in steady state under these conditions, which is a reasonable assumption, the rates of reactions (7), (8) and (4) must be equal, provided these are the only removal reactions for ClO, NO_2 and NO_3, i.e.

$$k_7[Cl] = k_8[ClO] = \tfrac{1}{2}k_4[NO_2] \qquad (iii)$$

and

$$[NO_3]_s = (k_5/4k_7)[ClONO_2] . \qquad (iv)$$

Although the steady-state absorption due to NO_3 increased with $[ClONO_2]$, the $[NO_3]_s$ values also exhibited a dependence on light intensity, which is not predicted by eq. (iv). This would arise if a [Cl]-independent loss route for NO_3 was present. The occurrence of such a loss route is indicated by the intercept on the plot in fig. 2 and the slow dark decay of NO_3. An approximate value of $4k_7/k_5 = 40 \pm 20$ could be obtained from the data, which is consistent with the value derived from fig. 2.

Information on the kinetics of the rate-determining step of the reaction sequence (7) + (8) + (4) can be obtained from the observed decay of NO_3 on cessation of photolysis. Close examination of fig. 1 shows that, on cessation of photolysis, NO_3 decays rapidly at first and then more slowly. Analysis of the decay from a number of experiments showed that the slow decay was first-order with a rate coefficient of 0.12 ± 0.03 s^{-1} independent of $[NO_3]_s$, i.e. similar to the intercept in fig. 2. This may be a wall-removal process or it may arise from decomposition of product N_2O_5 either thermally or photolytically, due to the unfiltered monitoring lamp beam.

In order to analyse the initial decay of NO_3, the log-linear portion of the NO_3 absorption decay curve was extrapolated back to t_0, corresponding to termination of photolysis, and the "excess" NO_3 removal was obtained by difference, as illustrated in fig. 3a. Fig. 3b shows a logarithmic plot of the "excess" NO_3 decay, which occurs with a half-life of 0.35 s and represents the time constant of the slowest, rate-determining step in the sequence (7) + (8) + (4).

The lifetime of Cl is determined by reaction (5) which, for the conditions in this experiment, gives $\tau_{Cl} = (k_5[ClONO_2])^{-1} = 0.43$ ms. Since $k_4 = 1.2 \times 10^{-12}$ cm^3 molecule^{-1} s^{-1} at 1 atm pressure and 296 K, $\tau_{NO_2} = (k_4[NO_3])^{-1} = 0.09$ s. Therefore, both Cl and NO_2 decay lifetimes are considerably shorter than the observed decay time for "excess" NO_3. It is concluded, therefore, that reaction (8) is the slowest step and it follows that ClO is the radical present at highest concentration. Assuming that the observed decay half-life of 0.35 s reflects the rate of reaction of ClO with NO_3 at an average concentration of 5.6×10^{12} molecule cm^{-3}, the observed rate gives $k_8 = 3.5 \times 10^{-13}$ cm^3 molecule^{-1} s^{-1}.

Neglecting the contribution due to Cl, which is only present at very low steady state ($\approx 3 \times 10^9$ molecule cm^{-3}), the "excess" NO_3 is related stoichiometrically to the steady states of ClO and NO_2 by

$$[NO_3]_e = 2[ClO]_s + [NO_2]_s . \qquad (v)$$

The steady-state relationships for $[ClO]_s$ and $[NO_2]_s$, eq. (iii), then give

$$k_8 = 2k_7[Cl]_s/([NO_3]_e - [NO_2]_s) .$$

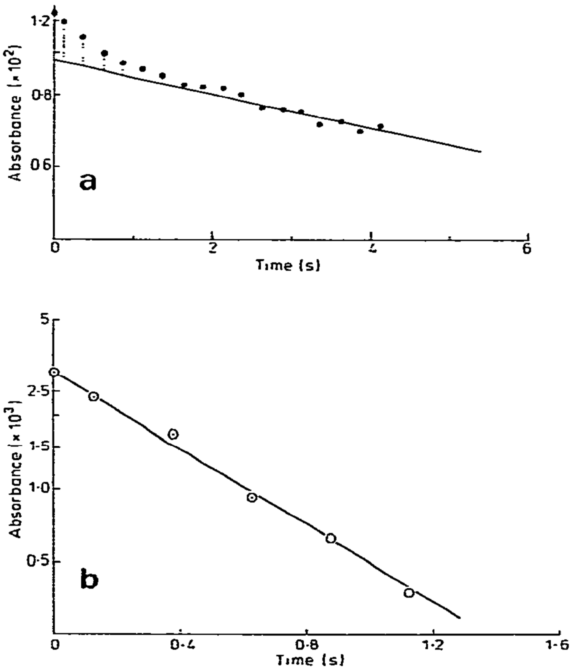

Fig. 3. (a) Decay of NO_3. (b) Decay of "excess NO_3" (from (a)).

Using the value of k_7 derived above and the experimental data in fig. 3, we obtain $k_8 = 3.6 \times 10^{-13}$ cm^3 molecule^{-1} s^{-1}, in excellent agreement with the absolute measurement from the "excess" NO_3 decay. Treatment of data sets from five separate experiments gave an average value of

$$k_8 = (4.0 \pm 1.6) \times 10^{-13}\ \text{cm}^3\ \text{molecule}^{-1}\ \text{s}^{-1}\ \text{at } 296\ \text{K}$$

(error = one standard deviation).

4. Discussion

The absorption cross section for NO_3 at 662 nm determined in the present work tends to support the higher values obtained by Marinelli et al. [4] and by Ravishankara and Wine [6]. The main sources of error were the determination of k_6 and measurement of overall concentrations of $[Cl_2]$, giving an estimated overall uncertainty of ±20%.

Kinetic data for reactions (7) and (8) have not been reported before. The value for k_7 is similar to the rate coefficient for the reactions of Cl with other radical species such as HO_2, OClO and ClOO, which are all $>10^{-11}$ cm^3 molecule^{-1} s^{-1}. The reaction of ClO with NO_3 is considerably slower, which is in accord with the lower reactivity of ClO compared to Cl, particularly with polyatomic species. An interesting analogy to reaction (8) is O transfer in the self-reaction of ClO:

$$\text{ClO} + \text{ClO} \rightarrow \text{ClOO} + \text{Cl}\,. \tag{10}$$

This reaction is also slow, $k_{10} \approx 3.5 \times 10^{-15}$ cm^3 molecule^{-1} s^{-1} at 298 K [12], the slow rate resulting from the endothermicity of the reaction (11.5 kJ mol^{-1}) and also the low A factor ($A_{10} \approx 3 \times 10^{-13}$ cm^3 molecule^{-1} s^{-1}). Since reaction (8) is exothermic and $k_8 \approx A_{10}$, reaction (8) may have near-zero activation energy and hence a very small temperature dependence.

The reactions of Cl and ClO with NO_3 comprise yet further coupling between the ClO_x and NO_x cycles in the chemistry of the stratosphere, and provide a sink for ozone through the reaction sequence

$$\text{Cl} + NO_3 \rightarrow \text{ClO} + NO_2\,,$$

$$\text{ClO} + NO_3 \rightarrow \text{Cl} + O_2 + NO_2\,,$$

$$2NO_2 + 2O_3 \rightarrow 2NO_3 + 2O_2\,,$$

$$\text{net } 2O_3 \rightarrow 3O_2\,.$$

This reaction scheme is unlikely to be a major influence on the O_3 budget, but it is of interest because it provides a route for converting the less reactive ClO species into Cl atoms during nighttime, when usual reaction partners O and NO, which result form photodissociation, are absent. Calculations using a one-dimensional atmospheric model with diurnal variations of photochemistry are needed for a quantitative assessment of the role of reactions (7) and (8) in the stratosphere.

Acknowledgement

This work was partly supported by the UK Department of the Environment.

References

[1] R.A. Cox and G.B. Coker, J. Atm. Chem. 1 (1983) 53.

[2] W.P.L. Carter, A.M. Winer and J.N. Pitts, Env. Sci. Technol. 15 (1981) 829.

[3] R.A. Graham and H.S. Johnston, J. Phys. Chem. 82 (1978) 254.

[4] W.J. Marinelli, D.W. Swanson and H.S. Johnston, J. Chem. Phys. 76 (1982) 2864.

[5] D.N. Mitchell, R.P. Wayne, P.J. Allen, R.P. Harrison and R.J. Twin, J. Chem. Soc. Faraday II 76 (1980) 785.

[6] A.R. Ravishankara and P.H. Wine, Chem. Phys. Letters 101 (1983) 73.

[7] M.J. Krylo, G.L. Knable and J.L. Murphy, Chem. Phys. Letters 95 (1982) 9.

[8] J.J. Margitan, J. Chem. Phys. 87 (1983) 674.

[9] R.A. Cox and D.W. Sheppard, J. Photochem. 19 (1982) 189.

[10] R.A. Cox and J.P. Burrows, J. Phys. Chem. 83 (1979) 2560.

[11] W.B. DeMore et al., Chemical Kinetics and Photochemical Data for use in Stratospheric Modelling, Eval. 6 NASA Panel for evaluation, J.P.L. Publication (1982) 383-62.

[12] R.A. Cox, R.G. Derwent, A.E.J. Eggleton and H.J. Reid, J. Chem. Soc. Faraday II 75 (1979) 1648.